

Remote Offshore Wind Farms (WFS) Connected Through Point-To-Point Dc Links

Naguru Ramadevi Satyam

M.Tech (EPS)

Arjun College of Technology and Science.

S. Vijay

Assistant Professor

Arjun College of Technology and Science.

ABSTRACT

Inertial reaction from remote seaward wind farms (WFs) associated through point-to-point DC joins depends on imitating of the coastal AC framework recurrence variety at each seaward wind turbine generator (WTG). This is not direct for a DC framework interconnecting WFs to different inland AC frameworks. To address this issue, this paper develops on a correspondence less approach already reported for arrangement of recurrence administrations from seaward WFs associated through a DC matrix. A weighted recurrence plan is received which depends on the fiber optic connection implanted inside the sub-ocean links for quick correspondence of on-shore recurrence varieties up to the seaward converters. The viability of the proposed methodology is indicated scientifically furthermore through a contextual investigation on a 4-terminal DC network interconnecting a seaward wind ranch and two coastal AC frameworks.

Index Terms—DC grid, droop control, frequency support, inertial response, offshore wind farm, voltage source converter (VSC)

I. INTRODUCTION

WIND force is prone to supplant a critical proportion of fossil-fuel based era in nations like the U.K. where around 17 GWs of seaward wind power limit are planned to be introduced by 2020 [1]. Dissimilar to routine synchronous force plants, wind ranches (WFs) don't actually contribute to framework inactivity. Substitution of a lot of synchronous machines with wind era would along these lines cause an intense decrease in the viable dormancy of future force frameworks. This would bring about huge

recurrence journeys and high rates of progress of recurrence (RoCoF) after an occasion like the departure of a creating unit, affecting the framework security and solidness [2]. Because of recurrence varieties, the WFs could be made to give inertial reaction through legitimate control. For instance, taking after a dunk in AC framework recurrence the wind turbines could be backed off to discharge the dynamic vitality put away in the turbine edges to reestablish the framework recurrence [3], [4]. Inertial backing from vast WFs will be basic for secure operation of low idleness frameworks without bounds [2].

For inland WFs and AC associated seaward WFs, singular wind turbine generators (WTGs) are synchronously associated with the principle lattice and can straightforwardly sense the varieties in AC framework recurrence to give inertial backing. In any case, remote seaward WFs are associated through a DC connection, which decouples the WF from the coastal AC framework. Recurrence varieties in coastal frameworks can never again be detected specifically by each WTGs. In such cases, the deliberate inland recurrence varieties can be imparted up to the seaward converter station to set the recurrence of the WF gathering system as needs be [5]. On the other hand, in a correspondence less plan, the inland recurrence variety could be copied at the WF through a relative variety in the DC join voltage utilizing a voltage-recurrence hang at both on-and seaward converters [6]–[8]. For a point-to-point DC association between the WF and the on-shore network, both of the above methodologies guarantees that individual WTGs can sense the copied variety in the on-shore lattice recurrence and give inertial backing.

Later on, WFs are liable to be associated with more than one coastal AC frameworks through a DC network taking into account voltage source converter (VSC) innovation [9] to expand the adaptability in operation and security of supply. For instance, a North - Sea lattice [10] and an European Supergrid [11] are visualized to permit compelling sharing of irregular renewable vitality sources between the European nations. Copying of inland framework frequencies at each WTG (required to give inertial backing) is not clear for seaward WFs associated with various coastal AC frameworks through a DC matrix. The test is to manage numerous recurrence varieties in various AC frameworks which could have inverse patterns [12]. Coastal converters inside a DC lattice can be controlled to permit trade of recurrence backing among the host inland AC frameworks. Utilization of recurrence voltage (-) hang control together with existing force voltage (-) hang control for independent force sharing [13] has been proposed in [14] and [15]. An option plan utilizing direct correspondence between the AC regions is accounted for in [16].

Be that as it may, there is not really any paper on the recurrence bolster arrangement from seaward WFs associated through DC lattices. Reference [17] is the first and ostensibly the main paper those arrangements with this particular issue: it proposes a correspondence less plan in light of utilization of hang control at both on-and seaward converters. The inland converter changes from - droop Building up on comparable thoughts as in [17] we propose a control methodology that uses the current rapid fiber optic connection em-slept with inside a sub-ocean link for conveying the coastal recurrence varieties up to the seaward converter stations of a DC framework. The recurrence references of the seaward converters are set to take after a weighted whole of the negative part of the coastal framework recurrence varieties in order to react just to under recurrence occasions. Hence the inland recurrence varieties are copied at the individual WTGs through the WF accumulation matrix setting off their inertial reaction. The technique works in con-

intersection with the current - and - hangs controllers employed at the coastal converter stations for self-sufficient force sharing and trade of recurrence backing. The adequacy of the proposed technique is assessed both logically and through a contextual investigation on a 4-terminal DC lattice interconnecting two host AC frameworks and a seaward WF.

II. DC GRID CONVERTER CONTROL

$Tof-V$ droop control at the point when a recurrence change is recognized at the relating AC framework. Along these lines recurrence support from seaward WFs could be given over a DC matrix together with trade of recurrence administrations among coastal AC frameworks. Be that as it may, there could be potential issues with force reference following and legitimate copying of inland recurrence deviations at the seaward WFs.

A. Control of Onshore Converters

As a characteristic expansion to indicate point HVDC joins, everything except one converter in a DC matrix can be controlled to keep up their particular reference power while the rest of the converter controls the DC join voltage, going about as a slack converter. If there should arise an occurrence of a converter blackout, just the slack converter will take up the whole share of the subsequent force irregularity. Also, the blackout of the slack converter will prompt the shutdown of the DC framework. Consequently utilization of force voltage (-) hang in every converter is prescribed as it permits every one of the converters to work in DC join voltage control mode keeping in mind the end goal to accomplish self-governing force sharing [18]. The estimation of the hang consistent impacts the sharing of the force awkwardness between the converters [13].

Counting an extra frequency-voltage ($f-V$) droop control on top of the $P-V$ droop permits trade of recurrence re-serves between the AC frameworks associated with the DC lattice [14], [15]. Fig. 1 demonstrates the single line chart of the coastal converter with decoupled control of the dynamic and

receptive force. Both P - V and f - V droop controllers are considered in are considered in the dynamic force control circle, which can be communicated scientifically as

$$V_{dc} = V_{dc}^{ref} - k_p(P_{dc} - P_{dc}^{ref}) + k_f(f - f^{ref})$$

Where k_p and k_f are the P - V and f - V droop constants, respectively. Note that the deliberate force is viewed as positive if the station goes about as a rectifier.

The nearness of a f - V droop not just permits trade of recurrence backing between the coastal AC frameworks but at the same time is important to effectively exchange the inertial reaction from the seaward WFs associated through a DC lattice. The extra power infused by the seaward WFs would be countervailed by the on-shore converters if just P - V droop control is set up, i.e., the force infused by the inland converters would change to attempt to adjust the surplus force inside the DC framework, diminishing the inertial backing from the WFs.

B. Control of Offshore Converters

The seaward converters associating the seaward twist ranches to the DC lattice are required to be controlled to exchange all the power the WFs are creating on to the DC matrix. Commonly, the seaward converters go about as hardened AC voltage sources which firmly direct the seaward AC voltage (V) at a given frequency (f_{off}) as appeared in Fig. 2 [19]. The seaward recurrence can be adjusted without fundamentally influencing the operation of the WF: as it is improbable that heaps will be associated specifically to the seaward framework, variable recurrence operation of the framework is conceivable [20].

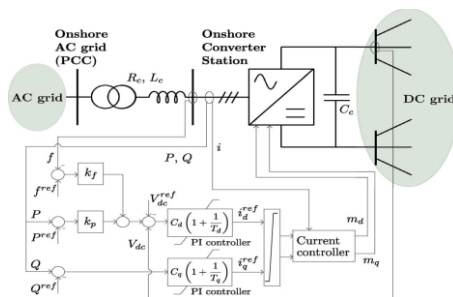


Fig. 1. Control of onshore converter

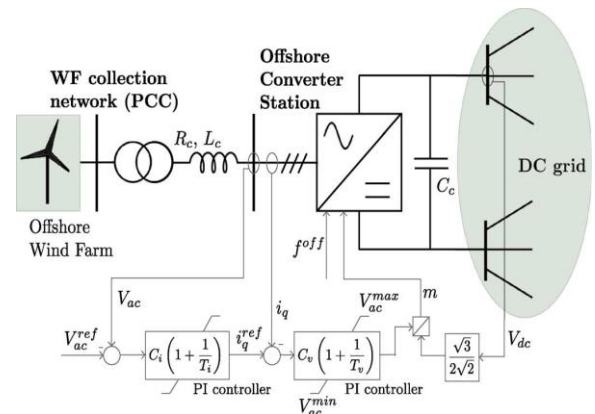


Fig. 2. Control of offshore converter.

III. WIND TURBINE GENERATOR (WTG) CONTROL

A. Basic Control

Variable pace wind turbines with completely evaluated converter (FRC) and perpetual magnet synchronous generator are considered in this study [21]. The control methodology for the FRC WTGs is appeared in Fig. 3. This incorporates the control circles for every converter, greatest force point following (MPPT) and pitch edge control to manage the force removed from the wind (P_W) which can be communicated as

$$P_W = \frac{1}{2} \rho \pi R^2 v_w^3 C_p(\beta, \lambda)$$

where ρ is the air density, R is the radius of the turbine, v_w is the wind speed and C is the power coefficient. C is dependenton the pitch angle β and the tip speed ratio λ , defined as $\lambda = \omega_r R / v_w$, where ω_r is the rotational speed of the turbine blades.

For low wind speed conditions, the wind turbine works in the supposed sub-appraised administration. The MPPT control modifies the rotor velocity to guarantee that the turbine works at the ideal tip speed proportion λ_{ot} , removing the most extreme force from the wind. The pitch edge is kept to 0_∞ , which compares to the most extreme force coefficients. Then again, for wind speeds over the evaluated one, the turbine works in the appraised administration with an expanded pitch edge (β) to restrain the turbine speed and output power at their evaluated values.

B. Inertial Control

The WFs can give recurrence support in two ways. Plausibility is to work as indicated by a deloaded ideal force removing bend [22]. On the other hand, brief overproduction can be accomplished through the arrival of the active vitality put away in the turbine edges by moderating the rate of the turbine [23] or pitching the edges [24]. In this paper we consider that the inertial reaction of the wind ranch does not rely on upon deloaded operation. There are a few systems for separating inertial reaction from WTGs [3], [25], [26]. Here we utilize the subsidiary of the recurrence varieties to change the force produced from the WTGs utilizing a first request channel after the $d\Delta f/dt$ input [3]:

$$\Delta P = K_I \frac{d\Delta f}{dt}$$

This specific work concentrates particularly on inertial reaction from seaward WFs associated through DC matrices. Nonetheless, the proposed structure is general furthermore applies to essential recurrence support from WFs with force save edge [27].

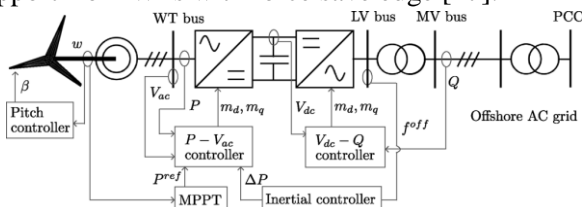


Fig. 3. Wind turbine generator (WTG) control.

IV. EMULATION OF ONSHORE FREQUENCY VARIATIONS AT OFFSHORE WIND TURBINE GENERATORS (WTGS)

In this section, two approaches for emulating the onshore frequency variations at the individual offshore WTGs across a DC grid are presented.

A. Communication-Less Scheme (CLS)

Keeping in mind the end goal to permit WFs associated through a point-to-point DC connection to take an interest in recurrence control, correspondence less plans have been proposed [6]–[8]. The inland converter creates an adjustment in DC join voltage

corresponding to the coastal recurrence variety utilizing a frequency- voltage (f - V) droop. Using a similar V - f droop, the offshore converter sets the frequency of the corresponding offshore WF collection net-work in proportion to the sensed DC voltage variation at the offshore end:

$$f^{off} = f^{ref} + k_{off}(V_{dc} - V_{dc}^{ref})$$

where k_{off} is a proportional term. This outcomes in flawless copying of inland recurrence at each WTG, if the hang constants are picked properly. A comparative plan was proposed in [17] with regards to seaward WFs associated with various on-shore AC frameworks through a DC lattice, from now on alluded to as Communication-Less Scheme (CLS). The CLS changes the recurrence of the seaward WF as indicated by (4). Be that as it may, as a DC lattice can have distinctive topologies and a few hang controllers, it is hard to appropriately copy the coastal recurrence varieties at each WF gathering system. This can be clarified from the expression for DC voltage at the seaward converter as de-rived next.

Give us a chance to consider a DC lattice with n converter stations where the n th one is the offshore converter station connected to an offshore WF while the remaining $(n-1)$ are onshore converter stations. Only one offshore converter is considered here for simplicity without any loss of generality.

The current injected i in the DC network by any converter i can be expressed as

$$I_{dc_i} = \sum_{j=1, j \neq i} G_{ij}(V_{dc_i} - V_{dc_j})$$

Where G_{ij} is the conductance of the line connecting stations i and j . We can re-write (5) for the offshore converter n . Grouping the constant terms and including the expression in (1) for V_{dc} , the offshore DC voltage can be expressed in terms of the variables in the $n-1$ onshore converters:

$$V_{dc_n} = e_n + \sum_{j=1}^{n-1} b_{nj} \left[V_{dc_j}^{ref} - k_{pj}(P_{dc_j} - P_{dc_j}^{ref}) + k_{fj}(f_j - f_j^{ref}) \right]$$

From (10) and (4) it can be seen that several factors, especially the term $k(P_{dc}-P_{ref})$, disturb the proportionality between onshore and offshore frequency variations. To deal with this, the CLS distinguishes between *normal* operation mode (only $P-V$ droop control in place, $k=0$) and *Disturbed operation* mode (only $f-V$ droop control in place, $k=0$) [17]. The *disturbed mode* is activated in a converter if the relating coastal recurrence deviation is outside a specific dead-band (e.g., mHz). This permits the arrangement of recurrence administrations over the DC lattice. In any case, there could be potential issues with force reference following and appropriate imitating of inland recurrence deviations at the seaward WFs because of the accompanying reasons, likewise outlined through reproduction comes about later in Section VII-A:

In normal operation, a change in power reference (P_{ref}) order to shift the infusions to/from the DC framework will aggravate the recurrence of the interconnected AC frameworks, setting off the bothered operation mode [17]. In this condition the force through the converter is not permitted to take after the reference summon, as the - hang control is removed from operation and the - hang control plans to keep up the recurrence of the framework.

The offshore DC voltage in (10) does not correspond to a proper weighted sum of onshore frequency variations, and the relative importance of each AC system frequency variation would be highly influenced by the DC grid topology and line resistances. In addition, a frequency event would not be reflected properly if each AC area is in a different operating mode (*normal* or *disturbed* [17]) or in the case of DC side disturbances (e.g., converter outage) that may lead to different frequency trends in the interconnected AC systems, as pointed out in [12].

Weighted Frequency Scheme (WFS)

Building up on the CLS, an alternative strategy that relies on fast communication of the onshore frequency variations up to the offshore converters is proposed in

this paper. The existing high speed fibre optic link embedded within a sub-sea DC cable is used for communication without any extra investment. The offshore frequency is set to follow the weighted sum of the on-shore AC system frequencies which is eventually reflected in the individual WTGs through the WF collection network. Thus the onshore frequency variations are properly emulated at each WTG, triggering their inertial response. Note that presence of fibre optics communication in every cable of the DC grid is not required, but there should exist at least one communication path from each onshore AC system to each offshore WF to ensure proper emulation of the frequency event in the offshore grid. The frequency in the offshore grid is shown in Fig. 4 and can be expressed as

$$f^{off} = f^{ref} + \sum_{j=1}^{2n_{on}} g_j (f_j - f_j^{ref})$$

Where g_j is a weight term for each $j=1,2,n_{on}$ corresponding to the onshore converter stations? We consider that the usual practice for the wind turbines (WTs) is to provide inertial support by reducing the turbine speed, which releases the stored kinetic energy to compensate for the lack of available power and thus support a low frequency event in the AC grid. Accordingly, as WFs are meant to provide inertial response for the under-frequency events only, the weight g_j is set to zero if the frequency variation in the j th AC system ($f_j - f_{ref}$) is positive. Additionally, the weight coefficients are chosen such that $\sum g_j = 1$. Situations in which the wind farm has to reduce its power output (i.e., WT speeding up and absorbing energy) that occur during fault-ride through (FRT) and periodic modulation of the WT power output for power oscillation damping are out of the scope of this study.

A worst-case time delay $T_{r=0.1s}$ is considered to model the latency in communication of onshore frequency variations. In reality, this fiber optic communication delay would be much less (of the order of 1–10 ms) for most of the time [28]. A dead band (± 10 mHz) is included to avoid re-responding to ambient frequency deviations.

It was shown in [12] that there are two distinct patterns of dynamic variations of the onshore frequencies in response to AC-side and DC-side disturbances. The onshore frequencies vary similarly for AC-side disturbance while, for a DC-side disturbance, the frequency of the affected system (where the event took place) varies in the opposite direction compared to the rest of the AC systems. Possible masking effect in the weighted sum due to opposite trends in onshore frequencies is accounted for by setting the corresponding weights to zero to respond only to under-frequency events (as described above). Clipping the positive variations in frequency ($f_j - f_{ref}$) in the CLS approach would affect the exchange of frequency support between on-shore AC systems. As a final remark, a combination of both CLS and WFS strategies could be exercised for certain scenarios, e.g., considering CLS to emulate frequency variations of onshore systems connected point-to-point in the WF offshore grid.

V. INERTIAL SUPPORT USING WEIGHTED FREQUENCY SCHEME (WFS)

An analytical formulation is presented in this section to show the effectiveness of WFS in reducing the negative frequency deviation in the onshore AC systems. We consider a generic framework in which each AC system i is connected to the DC grid by m_i converter stations and where the total number of AC systems is N . Equation (1) for the on-shore converter j expressed in small-signal form is

$$\Delta P_{dcj} = \Delta P_{dcj}^{ref} - \frac{1}{k_{pj}} \Delta V_{dcj} + \frac{k_{fj}}{k_{pj}} \Delta f_j$$

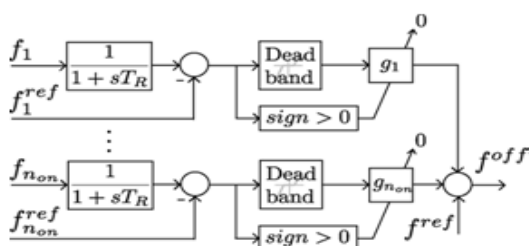


Fig. 4. Weighted frequency scheme (WFS) to emulate onshore frequency variations at offshore wind farms (WFs).

For the offshore converter j we derive a similar expression by using (3) and the offshore frequency defined by WFS in (11):

$$\Delta P_{dcj} \approx -K_I \frac{d\Delta f_j^{off}}{dt} = -K_I \sum_{j=1}^{n_{on}} g_j \frac{d\Delta f_j}{dt}$$

The total number of converters in the system is n , of which n_{on} are located onshore and n_{off} offshore connecting the WFs. Note that $\sum n_{mi} = n_{on}$ and $N \leq n_{on}$. If we neglect the change in DC grid losses, the sum of the exchanged power between the n converters of the DC grid is zero:

$$\sum_{j=1}^n \Delta P_{dcj} = \sum_{j=1}^{n_{off}} \Delta P_{dcj} + \sum_{j=1}^{n_{on}} \Delta P_{dcj} = 0$$

Considering that voltage drops at all converter terminals are comparable, we can derive an expression for DC voltage variations using (12) and (14):

$$\Delta V_{dc} = \sum_{j=1}^{n_{on}} k_{pj} \left(\sum_{j=1}^{n_{off}} \Delta P_{dcj} + \sum_{j=1}^{n_{on}} \Delta P_{dcj}^{ref} + \sum_{j=1}^n \frac{k_{fj}}{k_{pj}} \Delta f_j \right)$$

(15) Employing a classical first order power system model for frequency regulation studies, the power balance for each AC grid i is given by

$$2H_i \frac{d\Delta f_i}{dt} + D_i \Delta f_i = \Delta P_{Gi} - \Delta P_{Li} - \sum_{c_i} \Delta P_{dc_i}$$

Where the total active power demand in system A_i is the total generated power. D_i denotes the aggregated response of the governors in system, it yields

Substituting (12), (13) and (15) in (16) and considering, for simplicity, the same constant K_I in the control of all the offshore WFs, we obtain the following expression:

$$\begin{aligned} & \left(2H_i + \sum_{i=1}^{m_i} g_i n_{off} K_I g_i \right) \frac{d\Delta f_i}{dt} + \Delta P_{Li} \\ & = - \left(R_i + \sum_{i=1}^{m_i} \frac{k_{f_i}}{k_{p_i}} (1 - g_i) + D_i \right) \Delta f_i \\ & + \sum_{i=1}^{m_i} g_i \sum_{l=1, l \neq i}^{n_{on}} \left(\frac{k_{f_l}}{k_{p_l}} n_{off} K_I g_l \right) \frac{d\Delta f_l}{dt} \\ & - \sum_{i=1}^{m_i} (1 - g_i) \Delta P_{dc_i}^{ref} + \sum_{i=1}^{m_i} g_i \sum_{j=1}^{n_{on}} \Delta P_{dc_j}^{ref} \end{aligned}$$

Let us initially consider an AC side frequency event. From the above derivation we see that the inertial support from the off-shore WFs ($K_I > 0$) increases the effective inertia of system i by $\sum_{m \neq i} n_{off} K_I g_m$. In addition, the terms $n_{off} K_I g_m \Delta f_i / dt$ reduce the frequency variations in the interconnected AC systems caused by the frequency variation in system i . Therefore, the proposed WFS improves the transient frequency deviation of the onshore AC systems.

In case of a DC side frequency event in converter j connected to the onshore system i , an opposite trend in the frequency variation of this system with respect to the rest of onshore systems is expected, as seen in the last two terms on the right hand side of (17) and explained in [12]. As mentioned before, the elements g_j are greater or equal than 0, avoiding the participation in over-frequency events, which means that the inertia contribution from the offshore WFs would have an opposite effect in this system as compared to the rest of AC systems. Depending on the outraged converter operating mode (rectifier/inverter) the benefit in minimizing the frequency fall is obtained by either increasing the system inertia or reducing the coupling between onshore systems. Note that the above analysis is not dependant on the DC grid configuration and shows the benefit of WFS in a general framework. The simulation results shown later in Section VII are in agreement with this formulation.

VI. STUDY SYSTEM

The study system in Fig. 5 was adopted from [15] to illustrate the inertial support from offshore WFs connected through a DC grid. The 4-terminal DC grid interconnects three asynchronous AC systems: two onshore systems (System A and System B) and an offshore wind farm. System A is an interconnected AC system with two geographical regions [29] connected to the DC grid by converter stations #2 and #3. System B is modeled by a single equivalent generator, G5, connected to station #1. All the generators are conventional synchronous machines represented using the sub-transient model and equipped with both

governor control (steam turbine) and excitation system (IEEE-DC1A type) [30].

The DC grid is a general asymmetric bipole grid as in [13]. We consider a lumped parameter pi-section model for the DC cable network, consisting of positive, negative and metallic re-turn. The metallic return is only grounded at station #1 with a 0.5 Ω resistance and will carry the current in case of unbalanced operation in the system. The DC link voltage is ±350 kV and the AC systems are connected at 230 kV. Each converter station employs two 2-level VSC converters. Under nominal conditions, converter stations #1 and #4 act as rectifiers injecting active power into the DC grid, while #2 and #3 act as inverters. An offshore wind farm (WF) with a rated capacity of 1350 MW is connected at converter station #4. An aggregated model of the WTGs within the WF was used in the simulation. The WTG parameters were obtained from a simulation model in DIGSILENT PowerFactory, corresponding to a 1.5-MW permanent magnet synchronous machine, with radius of 30 m, 18 rpm rated speed and that enters the rated regime at 12.6 m/s. The following values were chosen in the simulations, conducted in DIGSILENT PowerFactory, for the droop controls in the on-shore converters: $r = 0.05$, and for the wind farm inertial controller: $K_I = 50$, $T_I = 1$ s. The droop constant values were chosen to strike a proper balance between conflicting objectives (adequate sensitivity vs. small DC link voltage variations) while ensuring the stability of the overall AC/DC grid system [13], [15].

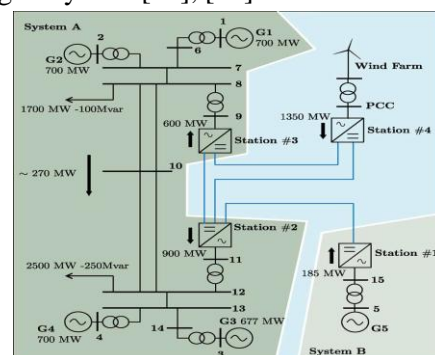


Fig. 5. 4-terminal DC grid interconnecting two onshore AC systems (Systems A and B) and an offshore wind farm (WF).

VII. SIMULATION RESULTS AND DISCUSSION

The simulation results in this section are presented under three categories. First the performance of the CLS is compared against the proposed WFS in terms of power reference tracking. The effectiveness of the WFS to enable the inertial response from offshore WFs is then demonstrated for both AC side load change events and also sudden change in power reference of an onshore converter. Lastly, the performance of the WFS is vali-dated under changing wind speed conditions.

A. Tracking of Power Reference Changes

For comparison, the CLS and the WFS were implemented separately at the offshore converter station #4. A step in the power reference at both positive and negative pole converters was considered to increase the injected power from 185 MW to 338 MW in station #1. The WF is assumed to operate in rated regime and produces 1350 MW.

Fig. 6(a) shows the frequency variation at the terminal of the onshore converter stations using the CLS. An opposing trend in the frequency variation of both AC systems can be observed which is typical for DC grid disturbances [12]. Clearly the CLS *disturbed* operation mode [17] (only *f-V* droop in place) is ac-tivated at all the onshore AC systems to maintain their corresponding frequency. It is to be noted that activation of the *f-V* droop control (*disturbed* mode [17]) in one onshore system disturbs the frequency of the other onshore systems which could also activate their *f-V* droop (and deactivate the *P-V* droop control), as shown in Fig. 6(a). The real power variation at

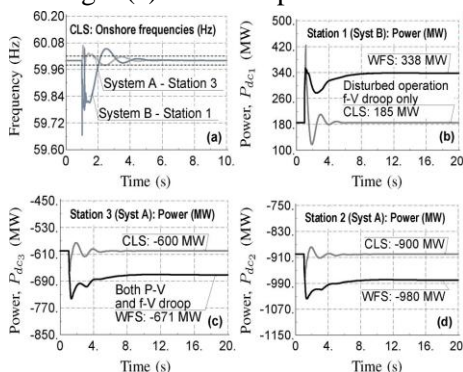


Fig. 6. System response after a step increase of real power reference at con-verter station #1. (a) Onshore AC system frequency variations using the CLS.(b)–(d) Power injections into the DC grid. Gray trace: with CLS; Black trace: with WFS.

the converter stations using the CLS (gray traces) is compared against the WFS (black traces) in subplots (b)–(d) of Fig. 6. For the CLS strategy, as a result of the *disturbed* mode [17] activation, the power exchanges are held at the same values as they were before the step change in power reference command was provided, see Fig. 6(b)–(d) (gray traces). On the other hand, the proposed WFS alters the power exchanges in response to the step change command with each onshore converter sharing the burden equally (black traces).

Note that the proposed WFS for inertial response from the WF is considered together with the presence of both *P-V* and *f-V* droop control loops at the onshore converters. The change in power reference required to achieve the desired power injection was factored into the control loops. Clearly, the ability of WFS to track power reference changes is one of the performance index for comparison against CLS.

B. Load Change in AC Systems

To demonstrate the effectiveness of inertial response using the WFS, a 40% step increase in the load connected at bus 8 in System A was considered. For this event the system response was investigated separately under high (19 m/s) and moderate (10 m/s) wind speed conditions. From here onwards, all the simulation results include *P-V* droop control at the onshore converters.

1) High Wind Speed Condition:

A constant 19 m/s windspeed is considered under which the WF operates in the rated regime producing 1350 MW. The turbines operate with pitch control to provide the rated power and avoid over speeding.

The frequency variations in System A and B are shown, respectively, in subplots (a) and (b) of Fig. 7. Without f - V droop (for exchange of frequency support between AC systems) on onshore converters, the frequency of System A measured near slack generator G3 (red traces) goes below 59.5 Hz with a maximum frequency excursion (frequency nadir) of 59.27 Hz [subplot (a)].

The frequencies of System B and the offshore WF are virtually unaffected as those systems are decoupled from System A in absence of f - V droop. With f - V droop on the onshore converters the frequency variation in System A (blue trace) is less than before. However, this comes at the expense of an acceptable (less than 0.3 Hz) frequency variation in System B. This is expected as the purpose of using the f - V droop is to exchange frequency support among the onshore AC systems [14], [15].

Activation of the WTG control for inertial response using the WFS improves the transient variation of the frequency (black trace) for both Systems A and B. Both the frequency nadir and the rate of change of frequency (RoCoF) are reduced. This is enabled by a properly emulated offshore frequency variation as shown by the black trace in Fig. 7(c) which closely resembles the actual frequency variations (black traces) in Systems A [Fig. 7(a)] and B [Fig. 7(b)]. The associated DC link voltage variations, shown in Fig. 7(d) are within the acceptable limits.

The frequency variations in Fig. 7 are driven by the power exchanges with the DC grid shown in Fig. 8. In the absence of f - V droop control (red traces), the power exchanged between the DC grid and the AC systems is not affected as they are decoupled. With only f - V droop control activated (blue traces) more power is injected through stations #2 and #3 into System A to supply the increased load. With a constant WF output (control for inertial response is not active), this extra power comes from System B.

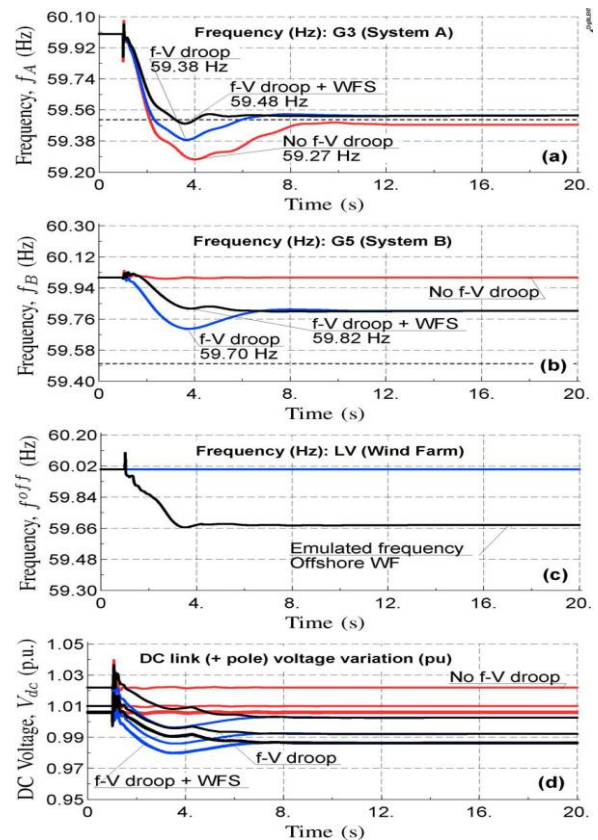


Fig. 7. System response after a step increase in load at bus 8 in System A under high wind speed condition. Red (light gray) trace: no f - V droop control at onshore converter stations; Blue (dark gray) trace: with f - V droop control; Black trace: with f - V droop and WFS for inertial response from WF.

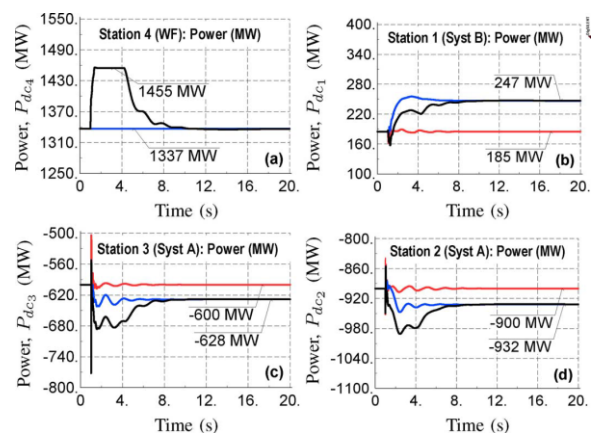


Fig. 8. Power injections into the DC grid after a step increase in load at bus 8 in System A under high wind speed condition. Red (light gray) trace:

no f - V droop control at onshore converter stations;
 Blue (dark gray) trace: with f - V droop control;
 Black trace: with f - V droop and WFS for inertial
 response from WF.

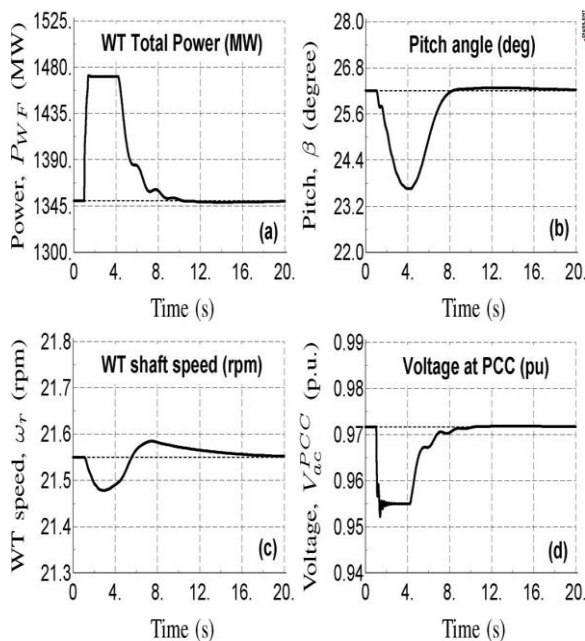


Fig. 9. Wind farm (WF) response with f - V droop and WFS for inertial re-sponse under high wind speed condition.

When both f - V droop control on onshore converters and the inertial control in the WTGs (black traces) are active, the re-release of inertial power (as shown in Fig. 8(a)) relieves the burden on System B by increasing the power injection into System A during the transient period, which improves the frequency variations in Fig. 7(a) and (b).

The aggregated response of the WF is plotted in Fig. 9. The inertial power is extracted by reducing the pitch angle [subplot (b)] with only a small change in the rotational speed of the turbine [subplot (c)].

Following inertial response the power output of the WF returns to the pre-disturbance level [subplot (a)]. The amount of such temporary over production would be limited by the short-term overload capability of the WTG components, especially

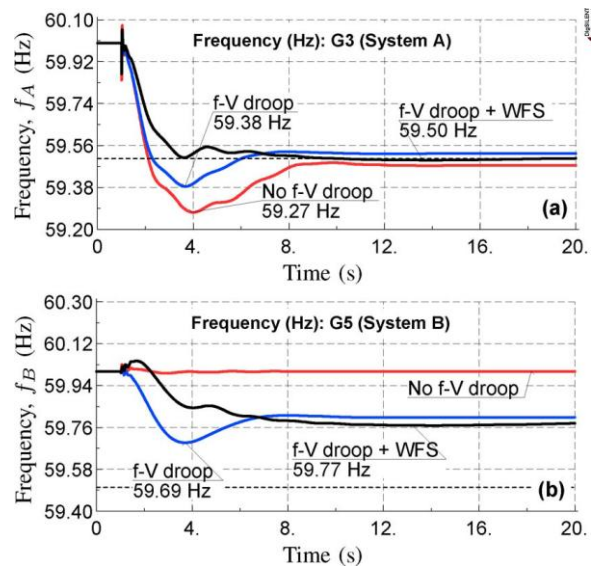


Fig. 10. Onshore AC system frequency variations after a step increase in load at bus 8 in System A under moderate wind speed condition. Red (light gray) trace: no f - V droop control at onshore converter stations; Blue (dark gray) trace: with f - V droop control; Black trace: with f - V droop and WFS for inertial response from WF.

the converters, and also by the DC grid converters. For this exercise, a 9% overload capacity in the tens of seconds time frame was assumed for the converters in the WT and the DC grid.

2) Moderate Wind Speed Condition: The same load event of the previous section is considered here under a moderate wind speed of 10 m/s. The WF operates in sub-rated regime and produces 680 MW. The turbine is controlled to operate at maximum power coefficient C_p while the pitch angle is kept constant at θ_0 .

As in the previous case the effectiveness of inertial control using the WFS is evident both in terms of improved RoCoF and frequency nadir as shown in Fig. 10. However, due to the recovery phase of the wind turbines, the restoration of post-event steady state is slower with a slight decrease of frequency observed after the initial support. The response of the WF operating in sub-rated regime is shown in Fig. 11. The inertial control extracts additional power from the WF

by slowing down the turbines [subplot (c)]. With decrease of the turbine speed, the MPPT control limits the turbine deceleration by reducing the power reference [subplot (b)]. Following the inertial support, there is a recovery phase before the turbines regain their original operating point after about 40 s. Note that we have considered an aggregated model of the WTGs to model the WF. In reality, the wind speed across all the turbines in the WF is not uniform due to wake effect [31]. As the considered inertial control is implemented at the wind turbine level, the individual WTG will react to frequency changes in its collection network to provide inertial support, experiencing different recovery periods depending on the wind speed present at the turbine.

C. Change of Converter Power Reference

In the previous section the effectiveness of inertial control using the WFS was illustrated for a load event within an onshore AC system. Here a disturbance within the DC grid is considered in the form of a step increase in the power reference at converter

its frequency goes down as shown in subplot (b). The frequency of System A (near generator $G3$) increases as shown in subplot (a).

This opposite trend in frequency variations is typical for DC grid disturbances as already mentioned in Section VII-A. The inertial support provided by the WF (black traces) improves the frequency nadir in System B compared to the case where only $f-V$ droop control is active on onshore converters (blue traces), see subplot (b). However, the additional inertial power injected by the WF causes a slight increase in the frequency of System A which is expected due to exchange of frequency support enabled by the $f-V$ droop control on onshore converters. In this case, the frequency variation in System B is emulated at the offshore WF [see subplot (c)] with no contribution from the positive frequency variation ($f_i - f_{ref}$) in System A.

D. Change of Wind Speed

A sudden change in the wind speed results in variations of on-shore AC system frequencies which would subsequently trigger inertial response from the WFs. To validate the control performance and the system transient response, we consider step changes to vary the wind speed. Although wind speed variations might be slower, step response simulations are interesting as they significantly affect the frequency of the onshore systems. The system response to such step changes in wind speed is shown in Fig. 13.

The presence of the inertial control using the WFS (black traces) improves the RoCoF and frequency nadir (which is not clear due to relatively long time scale) for both AC systems (System A and B) after the wind speed changes; see Fig. 13(a) and (b). This is achieved by reducing the turbine speed to provide the inertial support [subplot (c)]. It is to be noted that the WTG control adapts the rotor speed according to the wind speed to extract either the maximum power (sub-rated regime) or to operate at its rated value (rated regime), see

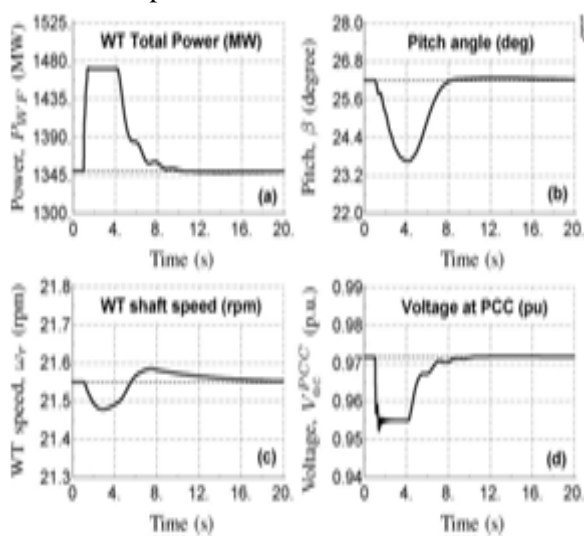


Fig. 11. Wind farm (WF) response with $f-V$ droop and WFS for inertial response under moderate wind speed condition.

station #1, same as in Section VII-A. The WF is assumed to operate at the rated regime producing 1350 MW. The system responses are shown in Fig. 12. As a result of the increased power export out of System B

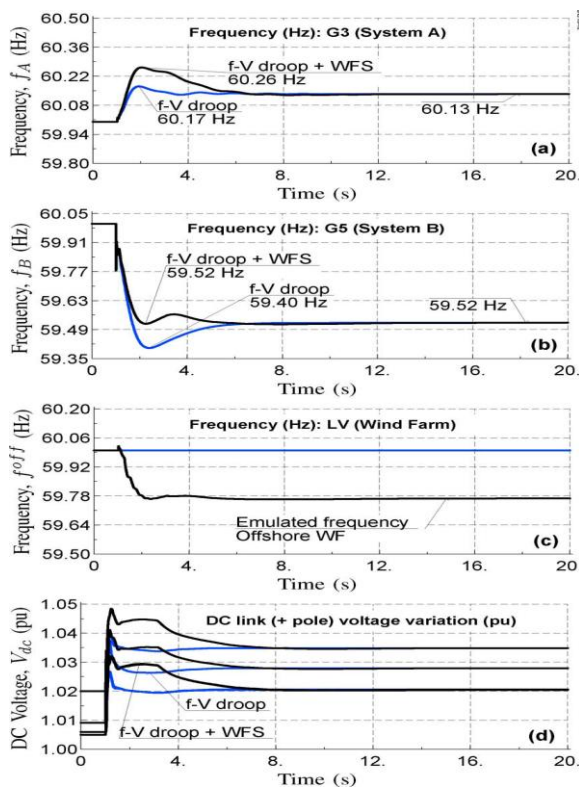


Fig. 12. System response after a step increase of real power reference at converter station #1 under high wind speed condition. Blue (dark gray) trace: with f - V droop control at onshore converter stations; Black trace: with f - V droop and WFS for inertial response from WF.

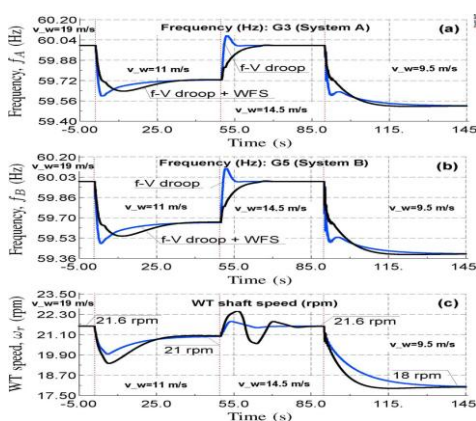


Fig. 13. System response to wind speed changes. Blue (dark gray) trace: with f - V droop control at onshore converter stations but no inertial response from WF; Black trace: with f - V droop and WFS for inertial response from WF.

subplot (c). For sub-rated regime ($v < 12.6 \text{ m/s}$), there is a recovery period following the inertial response which causes the frequency to go slightly below the one obtained with only f - V droop control.

VIII. CONCLUSION

A methodology for providing inertial response from offshore wind farms connected through a DC grid is demonstrated. As an extension to a communication-fewer schemes reported in the literature, this paper adopts an approach where the variations in onshore system frequencies are communicated to the off-shore converters using the fibre optic link embedded within the sub-sea DC cables. The analytical formulation presented in this paper shows the effective change in system inertia and frequency droop as a result of inertial support using the pro-posed WFS strategy. The case study on a 4-terminal DC grid connecting an offshore wind farm and two onshore AC systems also illustrates the inertial support from offshore WFs with the considered methodology. Different frequency events within the AC system and the DC grid were studied for varying wind speed conditions.

It is shown that the proposed WFS approach can improve the transient frequency deviation in the AC systems experiencing under- frequency problems which is critical for secure operation of low inertia systems of the future.

ACKNOWLEDGMENT

The authors would like to thank National Grid U.K. for technical inputs.

REFERENCES

1. Electricity Ten Year Statement (TYS), National Grid, 2012 [Online]. Available: <http://www.nationalgrid.com/uk/Electricity/ten-year-state-ment/current-elec-tys/>
2. G. Stein, Frequency Response Technical Sub-Group Report, National Grid, 2011 [Online]. Available: <http://www.nationalgrid.com/NR/>

rdonlyres/2AFD4C05-E169-4636-BF02-EDC67F80F9C2/50090/FRTSGGroupReportFinal.pdf

3. J. Ekanayake and N. Jenkins, "Comparison of the response of doubly fed and fixed-speed induction generator wind turbines to changes in network frequency," *IEEE Trans. Energy Convers.*, vol. 19, no. 4, pp. 800–802, Dec. 2004.

4. G. Lalor, A. Mullane, and M. O'Malley, "Frequency control and wind turbine technologies," *IEEE Trans. Power Syst.*, vol. 20, no. 4, pp. 1905–1913, Nov. 2005.

5. Z. Miao, L. Fan, D. Osborn, and S. Yuvarajan, "Wind farms with HVdc delivery in inertial response and primary frequency control," *IEEE Trans. Energy Convers.*, vol. 25, no. 4, pp. 1171–1178, Dec. 2010.

6. Y. Phulpin, "Communication-free inertia and frequency control for wind generators connected by an HVDC-link," *IEEE Trans. Power Syst.*, vol. 27, no. 2, pp. 1136–1137, May 2012

7. Y. Pipelzadeh, B. Chaudhuri, and T. C. Green, "Inertial response from remote offshore wind farms connected through VSC-HVDC links: A communication-less scheme," in *Proc. 2012 IEEE Power and Energy Soc. General Meeting*, Jul. 2012, pp. 1–6.

8. T. M. Haileselassie, R. E. Torres-Olguin, T. K. Vrana, K. Uhlen, and T. Undeland, "Main grid frequency support strategy for VSC-HVDC connected wind farms with variable speed wind turbines," in *Proc. 2011 IEEE Trondheim PowerTech*, Jun. 2011, pp. 1–6.

9. N. Flourentzou, V. G. Agelidis, and G. D. Demetriades, "VSC-Based HVDC power transmission systems: An overview," *IEEE Trans. Power Electron.*, vol. 24, no. 3, pp. 592–602, 2009.

10. J. Blau, "Europe plans a North Sea grid," *IEEE Spectr.*, vol. 47, no. 3, 12–13, 2010.

11. S. Gordon, "Supergrid to the rescue," *Power Engineer*, vol. 20, no. 5, 30–33, 2006.

12. I. MartínezSanz, B. Chaudhuri, and G. Strbac, "Frequency changes in AC systems connected to DC grids: Impact of AC vs. DC side events," in *Proc. 2014 IEEE Power and Energy Soc. General Meeting*, Jul. 2014, pp. 1–5.

13. N. R. Chaudhuri and B. Chaudhuri, "Adaptive droop control for effective power sharing in multi-terminal DC (MTDC) grids," *IEEE Trans. Power Syst.*, vol. 28, no. 1, pp. 21–29, Feb. 2013.

14. T. M. Haileselassie and K. Uhlen, "Primary frequency control of remote grids connected by multi-terminal HVDC," in *Proc. 2010 IEEE Power and Energy Soc. General Meeting*, Jul. 2010, pp. 1–6.

15. N. R. Chaudhuri, R. Majumder, and B. Chaudhuri, "System frequency support through multi-terminal DC (MTDC) grids," *IEEE Trans. Power Syst.*, vol. 28, no. 1, pp. 347–356, Feb. 2013.

16. J. Dai, Y. Phulpin, A. Sarlette, and D. Ernst, "Coordinated primary frequency control among non-synchronous systems connected by a multi-terminal high-voltage direct current grid," *IET Gener., Transm. Distrib.*, vol. 6, no. 2, pp. 99–108, Feb. 2012.

17. B. Silva, C. L. Moreira, L. Seca, Y. Phulpin, and J. A. Peças Lopes, "Provision of inertial and primary frequency control services using off-shore multiterminal HVDC networks," *IEEE Trans. Sustain. Energy*, vol. 3, no. 4, pp. 800–808, 2012.

18. J. Beerten and R. Belmans, "Analysis of power sharing and voltage deviations in droop-controlled DC grids," *IEEE Trans. Power Syst.*, vol. 28, no. 4, pp. 4588–4597, Nov. 2013.

19. S. Zhou, J. Liang, J. B. Ekanayake, and N. Jenkins, "Control of multi-terminal VSC-HVDC transmission system for offshore wind power generation," in *Proc.*

44th Int. Universities Power Eng. Conf. (UPEC),2009,
Sep. 2009, pp. 1–5.

20. X. Hu, J. Liang, D. J. Rogers, and Y. Li, “Power flow and power re-duction control using variable frequency of offshore AC grids,” *IEEETrans. Power Syst.*, vol. 28, no. 4, pp. 3897–3905, Nov. 2013.

21. A. Madariaga, J. Martín, I. Zamora, I. M. de Alegría, and S. Ceballos, “Technological trends in electric topologies for offshore wind power plants,” *Renew. Sustain. Energy Rev.*, vol. 24, pp. 32–44, 2013.

22. R. G. de Almeida and J. A. Peças Lopes, “Participation of doubly fed induction wind generators in system frequency regulation,” *IEEETrans. Power Syst.*, vol. 22, no. 3, pp. 944–950, Aug. 2007.

23. N. R. Ullah, T. Thiringer, and D. Karlsson, “Temporary primary fre-quency control support by variable speed wind turbines; potential and applications,” *IEEE Trans. Power Syst.*, vol. 23, no. 2, pp. 601–612, May 2008.

24. J. Conroy and R. Watson, “Frequency response capability of full con-verter wind turbine generators in comparison to conventional genera-tion,” *IEEE Trans. Power Syst.*, vol. 23, no. 2, pp. 649–656, May 2008.

25. J. Morren, J. Pierik, and S. W. de Haan, “Inertial response of vari-able speed wind turbines,” *Elect. Power Syst. Res.*, vol. 76, no. 11, pp. 980–987, 2006.